Unraveling the secrets of bacterial adhesion organelles using single-molecule force spectroscopy

Ove Axner, Oscar Björnham, Mickaël Castelain, Efstratios Koutris, Staffan Schedin, Erik Fällman, Magnus Andersson

Unraveling the Secrets of Bacterial Adhesion Organelles using Single Molecule Force Spectroscopy

Ove Axner*, Oscar Björnham[&], Mickaël Castelain*, Efstratios Koutris*, Staffan Schedin[&], Erik Fällman*[,#], and Magnus Andersson*

*Department of Physics, Umeå University, SE-901 87 Umeå, Sweden, and
[&]Department of Applied Physics and Electronics, Umeå University, SE-901 87 Umeå, Sweden.
[#]Deceased during the final preparation of the manuscript.

Abstract Many types of bacterium express micrometer-long attachment organelles (so called pili) whose role is to mediate adhesion to host tissue. Until recently, little was known about their function in the adhesion process. Force-measuring optical tweezers (FMOT) have since then been used to unravel the biomechanical properties of various types of pili, primarily those from uropathogenic *E. coli*, in particular their force-*vs.*-elongation response, but lately also some properties of the adhesin situated and the distal end of the pilus. This knowledge provides an understanding of how piliated bacteria can sustain external shear forces caused by rinsing processes, e.g. urine flow. It has been found that many types of pilus exhibit unique and complex force-*vs.*-elongation responses. It has been conjectured that their dissimilar properties impose significant differences in their ability to sustain external forces and that different types of pilus therefore have dissimilar predisposition to withstand different types of rinsing conditions. An understanding of these properties is of high importance since it can serve as a basis for finding new means to combat bacterial adhesion, including that caused by antibiotic-resistance bacteria. This work presents a review of the current status of the assessment of biophysical properties of individual pili on single bacteria exposed to strain/stress, primarily by the FMOT technique. It also addresses, for the first time, how the elongation and retraction properties of the rod couple to the adhesive properties of the tip adhesin.

Table of Contents

X.1 Introduction

Infections remain a major cause of mortality in the world. In particular, the widespread bacterial resistance to antibiotics is a ubiquitous and rapidly growing problem that needs to be addressed. There is therefore an urgent need for new antimicrobial drugs that can combat bacterial infections. It is a general consensus that the development of new drugs requires the identification of new targets in bacteria which, in turn, requires detailed knowledge of microbial pathogenic mechanisms. Since adhesion of bacterial pathogens to host tissue is a prerequisite for infection, the adhesion mechanism is one such possible target.

A bacterial infection starts in general with the adhesion of a bacterium onto a host cell. The adhesion mechanism has turned out to be far more complex than anticipated. For example, bacteria that express their adhesins directly on the cell wall are susceptible to shear forces. A shear flow will apply a torque onto the bacteria that will induce a successive breakage of bonds and result in bacterial rolling [1, 2]. This often implies that the bacteria detach from the host cell, which, in turn, makes it less likely that they can pursue their infectious task.

However, certain bacteria, and in particular those that are exposed to various types of rinsing processes, e.g. uropathogenic *E. coli* (UPEC), have developed adhesion organelles (pili) assembled on the cell walls to deal with shear forces. These pili are composed of a number of subunits, arranged in a helixlike arrangement in form of a rod. At the end of the helixlike rods, a short thin thread (tip fibrillum) is expressed, which anchors the adhesin that binds to the receptors expressed by host cells [3]. Moreover, UPEC bacteria can express different types of pilus. For example, P pili (pyelonephritis associated pilus, PAP) are a type that are expressed predominantly by isolates from the upper urinary tract [4, 5]; in fact, they are expressed by ~90% of the *E. coli* strains that cause pyelonephritis (severe urinary tract infection) [6]. Type 1 pili, on the other hand, are commonly found in the lower urinary tract and the bladder and can cause cystitis [7]. Both P and type 1 pili consist of a ~1 μm long and 6-7 nm diameter rod that is composed of $>10^3$ subunits of similar size, PapA and FimA for P and type 1 pili, respectively, arranged in a comparable higher order structure, *viz.* a right-handed helixlike arrangement with 3.28 and 3.36 subunits per turn, respectively [8, 9]. P pili have an adhesin known as PapG, which binds to galabiose, whereas the adhesin of type 1 pili is referred to as FimH, which binds to mannose [10, 11].

It was suggested in the mid-nineties that these organelles are expandable when exposed to a force [8]. It was later shown that the pili rod cannot only be significantly elongated by an unfolding process when exposed to force, it can also retract by a refolding process to its original length when no longer exposed to any force [12]. It has therefore been hypothesized that these adhesion systems may act as dynamic biomechanical machineries, enhancing the ability of bacteria to withstand high shear forces originating from rinsing flows, e.g. that of urine [1]. In particular, it has been conjectured that a large flexibility of the pili could allow for a redistribution of an external shear force among a large number of pili so each pilus

is exposed to a force that can be sustained by the adhesin, making the attachment organelles of crucial importance for the ability of bacteria to withstand rinsing actions. They thereby constitute an important virulence factor and a possible target for future anti-microbial drugs All this makes it important to assess the biophysical and biomechanical function of different types of attachment organelle, primarily their elongation and contraction properties, including the unfolding and refolding of the rod.

Static pictures of the pili structure can be obtained from conventional microscopy studies, e.g. using AFM or electron microscopy, and from crystallographic data, using X-ray diffraction [8, 9]. However, to obtain information about the dynamic properties of adhesion organelles, the biomechanical function of pili has to be probed in real time by studies under strain or stress. Moreover, bulk studies of bacteria will not give any detailed information about the function of an individual pilus, but rather an averaged ensemble behavior of all the pili involved [13]. In order to assess in detail the function of a given adhesion system, the elongation and contraction properties need to be assessed on a single pilus level (thus on an individual bacterial cell) under controlled conditions, primarily by an appropriately sensitive force measuring technique, capable of addressing a single macromolecule at a time. Thanks to the rapid development of sensitive force measuring techniques such studies can nowadays be performed. Several such studies have also been conducted lately, primarily by the authors, using force measuring optical tweezers (FMOT) [12, 14-24]. This work presents the status of the field and summarizes the present knowledge about the biophysical and biomechanical properties of individual pili on single bacterial cells, in particular their elongation, unfolding and refolding properties under strain. In addition, it addresses for the first time, how the elongation and retraction properties couple to the adhesive properties of the tip adhesin.

X.2 Instrumentation, Procedures, and Typical Force-*vs.*-elongation Response of Pili

X.2.1 Force Measuring Optical Tweezers - Instrumentation

Optical tweezers (OT) are a technique by which micrometer sized objects (inorganic as well as biological objects) can be trapped by well-focused laser light, by transfer of light momentum [25]. The basic principles of optical trapping and the first stable three-dimensional trap, based upon counter propagating beams, were established in the early 1970s by Arthur Ashkin [26, 27]. This made it possible to non-intrusively control and manipulate with great precision living biological objects in a fully controlled manner solely by light. A few years later the first single

gradient trap was completed and the optical tweezers technique, as we know it today, was born [28]. Since then, numerous groups worldwide have constructed and developed sensitive and user-friendly optical tweezers systems for optical micromanipulation [29].

Optical tweezers can also be used for force measurement in biological systems [30-34]. The basis is that the single gradient trap provides an attractive force (typically on the order of picoNewton, pN) on micrometer sized dielectrical particles (primarily non-absorbing particles with an index of refraction larger than that of the surrounding) that confines the particles in the focal region of the light. When an external force is applied to a trapped particle its position in the trap will shift due to force balance a distance F_{ext} / κ, where F_{ext} is the externally applied force and κ the stiffness of the trap. If the position of the bead in the trap is monitored, the force to which the bead is exposed at any given time can be assessed instantaneously. For force-*vs.*-elongation measurements, the bead thus acts both as a handle for the tweezers and a force transducer. For studies of adhesive properties, the bead also serves the purpose of carrying the receptor sugar to which the adhesin binds. The optical tweezers instrumentation used in this work has been described previously in the literature [35-37] and Fig. X.1A shows a schematic illustration of the set up.

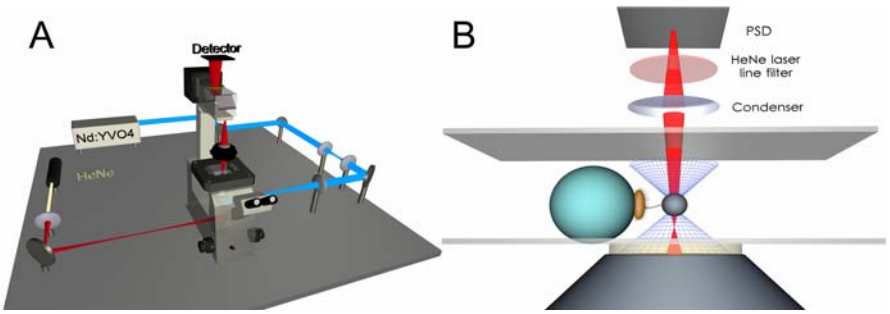

Fig. X.1. Panel A shows a schematic illustration of the force measuring optical tweezers (FMOT) system used by the authors. An inverted microscope has been modified for introducing of laser light for trapping (Nd:YVO_4) and probing (HeNe) through two side ports. The probing laser is fiber-coupled to reduce vibrations and to provide easy alignment. The trapping light is blocked by laser line filters so that only light from the probe laser reaches the PSD-detector. Panel B illustrates schematically the model system; a single bacterium is mounted on 9 um large bead firmly attached to the microscope slide. A trapped bead, to which one or several pili are attached, is used as a force transducer. The elongation is created by adjustments of the position of the microscope slide. The position of the trapped bead is probed by a probe laser. The deflection of the probe light is monitored by a position sensitive detector (PSD) whose output is converted to a force by a calibration process.

X.2.2 Experimental Procedure

The biological model system has been described in some detail previously [12]. In a typical experiment, an individual free-floating bacterium is trapped by the optical tweezers (run at low power, typically a few tenth of mW at the sample) and mounted on a large (9 μm) bead that is firmly attached to the microscope slide. A small free-floating bead (3 μm) is then trapped by the optical tweezers with normal power (a few hundreds of mW) and brought to a position close to but not in direct contact with the bacterium. The system is then calibrated by using the Brownian motion technique [38]. The small bead is subsequently brought close to the bacterium in order to achieve attachment between a few pili and the bead (Fig. X.1B). The piezo stage is then set in motion (at a constant speed) in order to provide a controlled elongation of the pilus/pili under study.

*X.2.3 Typical Force-*vs.*-elongation Response of Pili*

The experimental procedure produces in most cases multi-pili attachment, as is illustrated in Fig. X.2, which shows two typical force-*vs.*-elongation responses of *E. coli* pili. Panel A shows the response from a multitude of pili, whereas panel B illustrates the behavior from a single pilus. The black curves represent the response during elongation, whereas the grey curves correspond to contraction. Multi-pili responses will limit the amount of information that can be retrieved from the system since they will not give an unambiguous picture of the fundamental interactions in the system, primarily due to a partly unknown interplay between various pili. Single pilus experiments can be performed by first stretching the pili so detachment sets in. By then stopping when only one pilus is attached, and finally retracting the piezo-stage to the starting position, measurement on a single (and the same) pilus can then be performed a multitude of times.

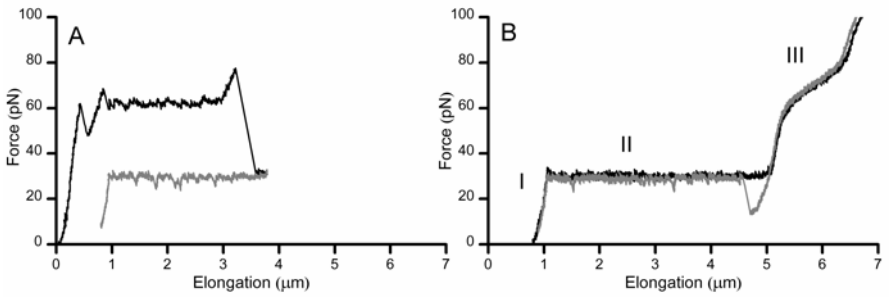

Fig. X.2. Panel A shows by the black line the force-vs.-elongation response of a multi-pili attachment. The binding is mediated by several pili for the first 0.5 μm of the elongation (black curve). From around 1 μm, the attachment is sustained by two pili elongated in region II. At around 3 μm, one pilus enters its region III, after which one pilus detaches. At around 3.5 μm,

only one pilus remains. The elongation is halted and reversed shortly thereafter. The retraction (gray curve) is mediated by a single pilus being in region I. Panel B shows a second elongation and contraction cycle of the same pilus, thus a pure single pilus force-vs.-elongation response.

Due to its structure, a pilus has an intricate force response that differs from that of a single bond as well as those of many other types of biopolymer. As is illustrated in Fig. X.2.B, a force-*vs.*-elongation response of a single pilus can be seen as composed of three regions; **Region I**, in which the response is basically linear, like that of a normal (elastic) spring; **Region II**, in which the force response is constant (elongation independent), like that of a material that undergoes plastic deformation; and **Region III**, in which the response has a monotonically increasing but non-linear force-*vs.*-elongation response.

Whereas the first region, in which the pilus is elongated a fraction of its length, can be understood as a general stretching of the pilus, but with no conformational change (no opening or closure of bonds), the other regions originate from the opening and closure of individual non-covalent bonds connecting the subunits in the pilus. As is schematically shown in Fig. X.3 (and further discussed below), the constant force-*vs.*-elongation response in region II is a direct result of an unfolding of the helixlike quaternary structure of the pilus by a *sequential* opening of the layer-to-layer bonds. The reason the opening of bonds is sequential in this region is that each layer of the quaternary structure consists of several bonds (slightly more than 3 subunits). Since each subunit can mediate one layer-to-layer bond, there are ~3 layer-to-layer bonds per turn [8]. When a pilus is exposed to a force, each bond in the interior of the rod will therefore experience approximately only one third of the applied force. The bond connecting the outermost unit in the folded part of the rod, on the other hand, experiences a significantly higher force, virtually the entire force to which the pilus is exposed. This implies that the outermost layer-to-layer bond of the rod will open significantly more often (or more easily) than a bond in the interior. Moreover, for an unfolding process in the interior of the rod to occur, three successive layer-to-layer bonds have to open simultaneously. Since this is a very rare process, the unfolding of the rod takes place predominantly by an opening of the outermost layer-to-layer bonds, which gives rise to a sequential opening procedure, sometimes referred to as a zipper like unfolding.

In contrast, the soft wave-like force-*vs.*-elongation behavior in region III originates from a stochastic conformational change of the bonds between consecutive subunits of the pilus in the linearized part of the rod (referred to as head-to-tail bonds). Since these bonds, which are composed by a donor strand interaction, can change (open and close) in a *random* manner, the particular shape of this region is governed by both properties of the individual bonds and entropy, of which the latter gives it its specific wave-like shape.

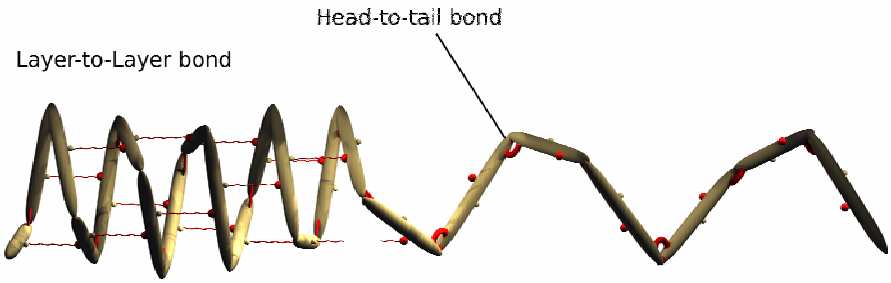

Fig. X.3. Schematic illustration of a pilus that is partly unfolded. The head-to-tail bonds, which holds consecutive subunits together and constitutes the backbone of the pilus rod, are marked with a thick arc whereas the layer-to-layer bonds, which are located between subunits in consecutive layers and hold the rod together, are illustrated by thin lines. Copyright Wiley-VCH Verlag GmbH & Co. KGaA. Reproduced with permission from Ref. [23].

In order to comprehend the adhesion properties of piliated bacteria it is necessary to acquire detailed information about the biophysical properties of individual pili under various conditions, in particular their behavior in region II and III, but also the adhesin on the tip of the pilus. Moreover, to understand the unfolding and refolding properties of the pilus rod a good knowledge about the properties of individual bonds exposed to strain/stress is needed. A full understanding of adhesion properties of piliated bacteria requires finally knowledge about how several pili cooperate to deal with an external force.

X.3 Theory

X.3.1 Bonds, Energy Landscapes, and Forces

X.3.1.1 Energy Landscape Representation of a Bond

As has been described previously in the literature [39], a non-covalent bond can be described in terms of an energy landscape, which is a representation of its energy-*vs.*-length dependence, consisting of at least two minima, representing the bond being “closed” and “open” (referred to as state A and B), respectively, and an intermediate local maximum, called the transition state (denoted by T). A closed bond can open, and thus elongate, only if it, somehow, “passes” this transition

state. The energy of the transition state, ΔV_{AT}, schematically illustrated in Fig. X.4, thereby represents the activation energy for bond opening. For an internal bond in a macromolecule, such as the layer-to-layer or the head-to-tail bonds in pili, state B is localized, whereas for a single external bond, e.g. that of an adhesin, it is non-localized.

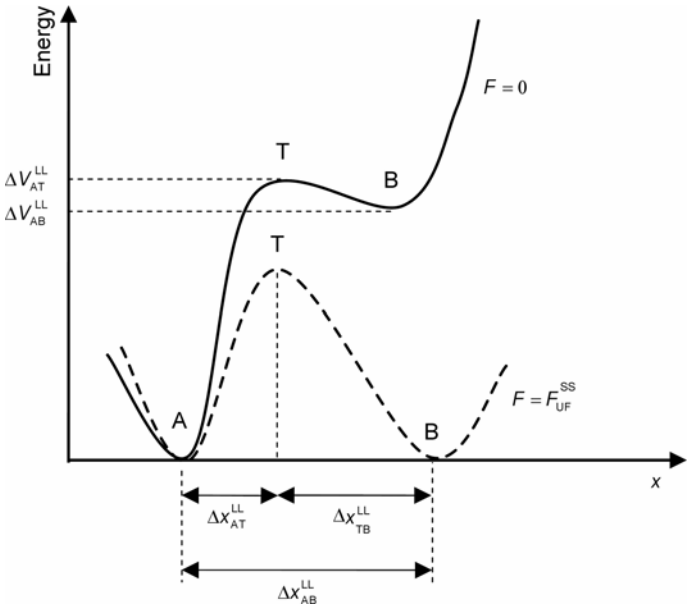

Fig. X.4. Schematic energy landscape diagram of a bond. The state A represents a closed bond whereas state B symbolizes an open. The position of the maximum of the energy landscape curve between the states A and B is referred to as the transition state, and is denoted by T. The uppermost curve represents the energy landscape for a bond not exposed to any force, whereas the lower refers to the case when the bond is exposed to a force equaling the opening and closure rates. The bond length, $\Delta x_{\mathrm{AT}}^{\mathrm{LL}}$, represents the distance from the minimum of state A to the transition state, whereas $\Delta x_{\mathrm{TB}}^{\mathrm{LL}}$ is the distance from the transition state to the minimum of state B. $\Delta x_{\mathrm{AB}}^{\mathrm{LL}}$ represents the total elongation of the bonds along the reaction coordinate when it opens.

X.3.1.2 Thermal Bond Dynamics

Due to the thermal energy, a bond will vibrate and each oscillation can be seen as an attempt to open. The bond opening rate can therefore, in general, be written as a product of an attempt rate, ν, and an Arrhenius factor, the latter encompassing the activation energy for opening the bond, i.e. as $\exp(-\Delta V_{\mathrm{AT}} / kT)$, where ΔV_{AT} is the difference in energy between an closed bond and the transition state, k is the Boltzmann constant and T the absolute temperature. A typical attempt rate for a bond in a liquid is around $10^9 - 10^{10}$ Hz whereas a typical activation energy

for a non-covalent bond can take values up to several tens of kT (which takes a value of 4 pN nm under room conditions) [40].

An open bond in the localized B state can subsequently close. Also the closure rate will take place with a rate given by the product of the attempt rate and an Arrhenius factor, this time encompassing the difference in energy between the transition state and the open state, i.e. $\exp[(-(\Delta V_{\mathrm{AT}} - \Delta V_{\mathrm{AB}})/kT]$, where ΔV_{AB} is the difference in energy between an open and closed bond.

X.3.1.3 A Single Bond Exposed to a Force

Applying a force to a bond (often called stress in the world of biophysics) alters the activation barriers and thereby also the bond opening and closure rates, which in turn affects the behavior of the bond [39-43]. This is the basis for force spectroscopy of bonds. The activation energy for bond opening is lowered by an amount equal to the product of the force and the bond length (the latter given by the distance from the closed state to the transition state), i.e. by an amount of $F\Delta x_{\mathrm{AT}}$. The activation energy for bond closure is similarly increased an amount equal to the product of the force and the length between the transition state and the open state, i.e. by $F\Delta x_{\mathrm{TB}}$ [39]. This is usually envisioned as if the energy landscape is tilted with a slope given by the force, as is illustrated by the dashed curve in Fig. X.4. The closure rate for a single bond with a non-localized "open" state exposed to an external force is most often negligible.

X.3.1.4 Dynamics of a Single Bond Exposed to a Force

Due to the statistical properties of thermodynamics, a single bond, exposed to an increasing force a number of consecutive times, will open at a broad distribution of forces, of which the peak position is called the bond strength [40, 44]. For a soft force transducer, the force applied to the bond can be written as $\Delta L\kappa$ where ΔL is the distance the force transducer has been moved. When the distance is increased with a given speed, $\dot{L}$, a single bond will be exposed to a linearly increasing force, given by $\dot{L}\kappa$, referred to as the loading rate. As is further discussed below, a bond exposed to a constant loading rate will experience a progressively increased probability for opening. The integrated history of such a time dependent opening probability determines the fate of the bond. This implies that the strength of a single bond will depend on the loading rate and thereby also the elongation rate. It can be shown that, under a set of fairly normal conditions, the strength of a single bond is proportional to the logarithm of the loading rate (or the elongation speed) whereas the slope provides information about the bond length [39-44].

X.3.1.5 Sequential Bond Dynamics

In contrast, if a macromolecule consists of several bonds that are arranged in a sequential configuration of parallel bonds, as is the case for a helixlike structure, the width of the bond opening distribution is decreased by a force stabilizing process and all bonds will open in succession at more or less the same force, which, in turn, gives rise to a force plateau in the force-*vs.*-elongation response [12, 17, 45]. As is discussed further below, the value of this force depends, under some conditions, on the elongation speed; it is fairly independent of the elongation speed for low speeds, but proportional to the logarithm of the elongation speed for higher speeds.

X.3.2 Rate Theory for Unfolding and Refolding of a Helixlike Polymer Exposed to Strain or Stress – Pili Elongated in Region II

X.3.2.1 Opening and Closure Rates of an Individual Bond

The net opening rate of the outermost layer-to-layer (LL) bond in the folded part of a helixlike polymer exposed to a force, F, defined as the number of times a layer-to-layer bond opens per unit time, $k_{\mathrm{AB}}^{\mathrm{LL,net}}(F)$, can be written as the difference between the bond opening and the bond closure rates under the exposed stress, i.e. as $k_{\mathrm{AB}}^{\mathrm{LL}}(F) - k_{\mathrm{BA}}^{\mathrm{LL}}(F)$, which, in turn, can be expressed as [39]

$$k_{\mathrm{AB}}^{\mathrm{LL}}(F) = k_{\mathrm{AB}}^{\mathrm{LL,th}} e^{F\Delta x_{\mathrm{AT}}^{\mathrm{LL}}/kT} \tag{X.1}$$

and

$$k_{\mathrm{BA}}^{\mathrm{LL}}(F) = k_{\mathrm{AB}}^{\mathrm{LL,th}} e^{(\Delta V_{\mathrm{AB}}^{\mathrm{LL}} - F\Delta x_{\mathrm{TB}}^{\mathrm{LL}})/kT}, \tag{X.2}$$

where $k_{\mathrm{AB}}^{\mathrm{LL,th}}$ is the thermal bond opening rate in the absence of force. $\Delta x_{\mathrm{AT}}^{\mathrm{LL}}$ and $\Delta x_{\mathrm{TB}}^{\mathrm{LL}}$ are the distances between the closed state A and the transition state T, and between the transition state T and the open state B for the layer-to-layer bond, respectively, where the former often is called the bond length. These expressions are sometimes referred to as Bell's equations for unfolding and refolding [39].

X.3.2.2 The Rate-equation for Bond Opening and Bond Closure in Region II

Due to the sequential mode of opening and closure, the bond opening rate of region II, defined as the number of bonds that open per unit time, dN_B / dt, where N_B is the number of open layer-to-layer bonds at any given time, is identical to the net opening rate of the outermost bond, $k_{AB}^{LL,net}(F)$. This implies that the bond opening rate of region II can be expressed as a rate-equation according to

$$\frac{dN_B}{dt} = k_{AB}^{LL}(F) - k_{BA}^{LL}(F) . \tag{X.3}$$

X.3.2.3 The Rate-equation for the Force in the System

Owing to the experimental procedure, the force in the system, F, can be related to the forced elongation speed of the pili, $\dot{L}$, and the bond opening rate, dN_B / dt, according to

$$\frac{dF}{dt} = \left(\dot{L} - \frac{dN_B}{dt} \Delta x_{AB}^{LL} \right) \kappa . \tag{X.4}$$

where Δx_{AB}^{LL} is the bond opening length, defined as $\Delta x_{AT}^{LL} + \Delta x_{TB}^{LL}$ [17].

Information about the force-*vs.*-elongation-speed-behavior of a helixlike polymer, $F_{II,UF}(\dot{L})$, unfolding at a constant force, can then be obtained by solving the Eqs (X.3) and (X.4) for $dF / dt = 0$. Equation (X.4) then shows that the (forced) bond opening rate, dN_B / dt, is equal to the ratio of the elongation speed and the bond opening length, i.e. $\dot{L} / \Delta x_{AB}^{LL}$. Solving Eq. (X.3) under such conditions gives rise to a force-*vs.*-elongation-speed-behavior that is schematically illustrated in Fig. X.5A.

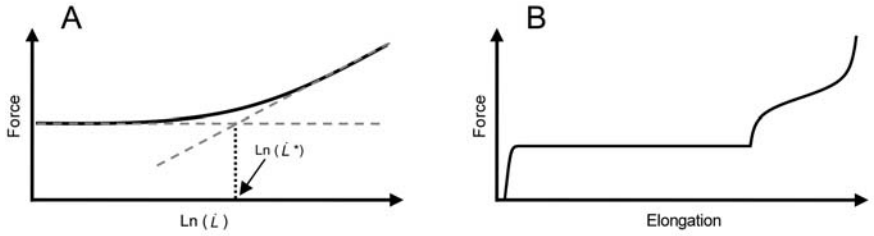

Fig. X.5. Panel A gives a schematic illustration of the force response of a helixlike biopolymer (pili in region II) as a function of elongation speed. Panel B illustrates a numerical simulation of the rate equations for elongation of a pilus under steady-state conditions.

X.3.2.4 Unfolding and Refolding under Steady-state Conditions

As can be seen from the figure, for low speeds, up to the so-called corner velocity, $\dot{L}^*$, given by [12]

$$\dot{L}^* = \Delta x_{\mathrm{AB}}^{\mathrm{LL}} k_{\mathrm{AB}}^{\mathrm{LL,th}} e^{(\Delta x_{\mathrm{AT}}^{\mathrm{LL}} / \Delta x_{\mathrm{AB}}^{\mathrm{LL}}) V_{\mathrm{AB}}^{\mathrm{LL}} / kT}, \tag{X.5}$$

the force at which the rod unfolds depends only weakly on the elongation speed. For such elongation speeds, there is a balance between the bond opening and the bond closure rates, both being larger than the forced bond opening rate; in particular the bond closure rate is larger than the forced bond opening rate, i.e., $k_{\mathrm{BA}}^{\mathrm{LL}}(F) > dN_{\mathrm{B}}/dt$. This implies that each bond will open and close several times with similar rates, $k_{\mathrm{AB}}^{\mathrm{LL}}(F) \approx k_{\mathrm{BA}}^{\mathrm{LL}}(F)$, which often are referred to as the balance rate, $k_{\mathrm{AB}}^{\mathrm{LL,bal}}$, before the neighboring bond starts to open. Measurements performed under such conditions are therefore referred to as being done at under steady-state conditions. Under such conditions, Eq. (X.3) gives rise to an expression for the steady-state unfolding force of a helixlike polymer (i.e. a pilus in its elongation region II), $F_{\mathrm{II,UF}}^{\mathrm{SS}}$, that reads

$$F_{\mathrm{II,UF}}^{\mathrm{SS}} = \Delta V_{\mathrm{AB}}^{\mathrm{LL}} / \Delta x_{\mathrm{AB}}^{\mathrm{LL}}. \tag{X.6}$$

This shows that under low-speed conditions, the force is (virtually) independent of the elongation speed and solely given by energy landscape parameters. This also implies that the refolding force, $F_{\mathrm{II,RF}}^{\mathrm{SS}}$, is similar to the unfolding rate.

X.3.2.5 Unfolding and Refolding under Dynamic Conditions

For higher elongation speeds, on the other hand, i.e. those above $\dot{L}^*$, the forced bond opening rate, dN_{B}/dt, becomes larger than the bond closure rate, $k_{\mathrm{BA}}^{\mathrm{LL}}(F)$. The closure rate can therefore be neglected whereby the bond opening rate, $k_{\mathrm{AB}}^{\mathrm{LL}}$, is in direct balance with the forced elongation opening rate, $\dot{L} / \Delta x_{\mathrm{AB}}^{\mathrm{LL}}$. Solving the Eqs (X.3) and (X.4) under these conditions gives rise to an expression that relates the unfolding force in region II under dynamic elongation conditions, $F_{\mathrm{II,UF}}^{\mathrm{DFS}}$, to the elongation speed in an logarithmic manner, *viz.* as

$$F_{\mathrm{II,UF}}^{\mathrm{DFS}}(\dot{L}) = \frac{kT}{\Delta x_{\mathrm{AT}}^{\mathrm{LL}}} \ln\left(\frac{\dot{L}}{\Delta x_{\mathrm{AB}}^{\mathrm{LL}} k_{\mathrm{AB}}^{\mathrm{LL,th}}} \right). \tag{X.7}$$

Force measurements made under these conditions are commonly referred to as dynamic force spectroscopy (DFS). The advantage with DFS measurements is that it is possible to assess values to physical entities that cannot be addressed by mea-

surements under steady-state conditions, predominantly those related to the transition state, i.e. $\Delta x_{\mathrm{AT}}^{\mathrm{LL}}$ and $k_{\mathrm{AB}}^{\mathrm{LL,th}}$ [12, 46, 47].

Under dynamic conditions, the refolding force, $F_{\mathrm{II,RF}}^{\mathrm{DFS}}$, is lower than the unfolding force under steady-state as well as dynamic conditions [45].

X.3.2.6 Unfolding under Relaxation Conditions

As an alternative to dynamic force spectroscopy, it is possible to monitor the decay in force that follows when the elongation of the pilus is suddenly halted. This is particularly useful for the cases when the corner velocity is low, as is the case for type 1 pili (see further discussion below). An expression for the unfolding force from an elongated pilus that is suddenly halted can be derived from the Eqs (X.3) and (X.4) under the condition that $\dot{L} = 0$. Again under the condition that the refolding rate can be neglected, the resulting expression becomes a separable differential equation from which an expression of the decaying unfolding force under dynamic relaxation conditions (DRC), $F_{\mathrm{II,UF}}^{\mathrm{DRC}}(t)$, can be derived [23],

$$F_{\mathrm{II,UF}}^{\mathrm{DRC}}(t) = -\frac{kT}{\Delta x_{\mathrm{AT}}^{\mathrm{LL}}} \ln\left[e^{-F_{\mathrm{II,UF}}^{0}\Delta x_{\mathrm{AT}}^{\mathrm{LL}}/kT} + \frac{\Delta x_{\mathrm{AB}}^{\mathrm{LL}} \kappa \Delta x_{\mathrm{AT}}^{\mathrm{LL}}}{kT} k_{\mathrm{AB}}^{\mathrm{LL,th}} t \right], \qquad \text{(X.8)}$$

where $F_{II,UF}^{0}$ is the initial force at the time when the elongation is halted and t is the time thereafter. This expression thus describes the force-*vs.*-time response of a helixlike biopolymer when the applied elongation is suddenly halted. The actual form of this expression is shown below as fits to measurements.

X.3.3 Rate Theory for Elongation and Contraction of a Linear Polymer Exposed to Strain or Stress – Pili Elongated in Region III

X.3.3.1 The Rate-equation for Bond Opening and Closure in Region III

The elongation of a linearized pilus, i.e. when the entire helixlike structure has been unfolded and the pilus resides in Region III, differs from that of a helixlike structure in the respect that all bonds have the same probability to open and close, irrespectively of their neighbors. Region III is therefore governed by a set of random transitions between the closed and opened states of the head-to-tail bonds, referred to as states B and C, respectively. The randomness implies that the bond opening rate is strongly affected by entropy, which gives it its soft wave-like form, sometime referred to as entropic softening. The head-to-tail (HT) bond opening

rate in the linearized configuration (region III), dN_C / dt , can thereby be described by the rate equation,

$$\frac{dN_C}{dt} = N_B k_{BC}^{HT}(F) - N_C k_{CB}^{HT}(F), \tag{X.9}$$

where N_B and N_C are the number of closed and opened head-to-tail bonds, respectively, and where the bond opening and closure rates are similar to those defined in Eq. (X.3).

Inasmuch as all bonds are involved in the length regulation of region III (and not solely the outermost bond of the folded part of the rod as is the case for region II), the dynamic region is entered whenever $\dot{L} / \Delta x_{BC}^{HT} > N_C k_{CB}^{HT}(F)$. Since $N_C \gg 1$ (N_C is in most cases ~10^3), the onset of the dynamic response in region III takes place at a significantly higher speed than in region II. Region III can therefore be considered to be in its steady-state region for the entire range of speeds examined.

X.3.3.2 Steady-state Conditions

Under steady-state conditions the force response of region III can be written as

$$F_{III}^{SS} = \frac{\Delta V_{BC}^{HT}}{\Delta x_{BC}^{HT}} + \frac{kT}{\Delta x_{BC}^{HT}} \ln\left(\frac{N_{TOT} - N_B}{N_B}\right), \tag{X.10}$$

where ΔV_{BC}^{HT} and Δx_{BC}^{HT} are the difference in energy between an open and closed head-to-tail bond (in the absence of stress) and the bond opening length, respectively, and N_{TOT} and N_B are the total number of units in the rod and the number of closed head-to-tail bonds in the linearized pili, respectively. Since the length of the pilus, L , can be related to N_{TOT} and N_B by geometrical means, Eq. (X.10) provides an expression for the force-*vs.*-elongation (as well as the force-*vs.*-contraction) behavior of pili in region III under steady-state conditions [16-18]. Although not explicitly evident from the derivation given above, the expression given in Eq. (X.10) includes the softening effect of entropy [12].

The fact that region III most often is in its steady-state regime implies that some energy landscape parameters for the head-to-tail bond, e.g. Δx_{BT}^{HT} and ΔV_{BT}^{HT} , cannot readily be assessed.

*X.3.4 Predicted Force-*vs.*-elongation Response of a Single Pilus*

As was illustrated above, the rate equation for the force, Eq. (X.4), can, together with the rate equations for bond opening and closure, Eqs (X.3) and (X.9), and

Bell's equations for unfolding and refolding, Eqs (X.1) and (X.2), be solved analytically under steady-state conditions, for the regions II and III, respectively, giving rise to the Eqs (X.6) and (X.10). This behavior is schematically illustrated in Fig. X.5B. As can be seen by a direct comparison with the force-*vs.*-elongation response of a single pilus shown in Fig. X.2B, the agreement is good.

However, it is not as simple to provide an expression for the force-*vs.*-elongation behavior under general conditions, in particular not for non-constant elongation speeds or elongation speeds in proximity of the corner velocity (i.e. for $\dot{L} \approx \dot{L}^*$). The reason is that analytical solutions can only be found under steady-state conditions or if the refolding rate is neglected, which are good approximations when $\dot{L} < \dot{L}^*$ and $\dot{L} > \dot{L}^*$, respectively [12]. Under such conditions, the force-*vs.*-elongation behavior of a helixlike polymer (i.e. a pilus in region II) is given either by Eq. (X.6) or (X.7). The dynamic response in the intermediate range needs therefore to be solved numerically, e.g. by numerical integration, or can be found by Monte-Carlo simulations [22].

X.3.5 Pili Detachment under Exposure to Stress

A pilus will detach from its receptor on the host cell whenever the adhesin bond opens. As was shown by Eq. (X.1), also the opening rate for the adhesin (Ad) bond, $k_{\mathrm{AB}}^{\mathrm{Ad}}(F)$, depends exponentially on the force to which it is exposed. Since the adhesin is located on the tip of the pilus, the force to which it is exposed is that exerted by the rod, which for a single pilus attachment is equal to the external force.

It has been found that the lifetime of an adhesin is rather long (> 1 s) for forces below the steady-state unfolding force, $F_{\mathrm{II,UF}}^{\mathrm{SS}}$ [48]. This implies that it is reasonable to assume that the adhesin bond will remain closed as long as the pilus is elongated in region I.

In elongation region II, the force to which the adhesin is exposed is equal to the unfolding force, $F_{\mathrm{II,UF}}$. This implies that the bond opening rate for the adhesin, $k_{\mathrm{AB}}^{\mathrm{Ad}}(F)$, can, for the two cases with slow or fast elongation (i.e. for $\dot{L} < \dot{L}^*$ and $\dot{L} > \dot{L}^*$, respectively), be written as

$$k_{\mathrm{AB}}^{\mathrm{Ad}}(F) = k_{\mathrm{AB}}^{\mathrm{Ad,th}} e^{F_{\mathrm{II,UF}}^{\mathrm{SS}} \Delta x_{\mathrm{AT}}^{\mathrm{Ad}} / kT} = k_{\mathrm{AB}}^{\mathrm{Ad,th}} e^{(\Delta x_{\mathrm{AT}}^{\mathrm{Ad}} / \Delta x_{\mathrm{AB}}^{\mathrm{LL}}) \Delta V_{\mathrm{AB}}^{\mathrm{LL}} / kT} \qquad \text{(X.11)}$$

and

$$k_{\mathrm{AB}}^{\mathrm{Ad}}(F) = k_{\mathrm{AB}}^{\mathrm{Ad,th}} e^{F_{\mathrm{II,UF}}^{\mathrm{FDS}} \Delta x_{\mathrm{AT}}^{\mathrm{Ad}} / kT} = k_{\mathrm{AB}}^{\mathrm{Ad,th}} \left(\frac{\dot{L}}{\Delta x_{\mathrm{AB}}^{\mathrm{LL}} k_{\mathrm{AB}}^{\mathrm{LL,th}}} \right)^{\rho}, \qquad \text{(X.12)}$$

respectively, where $k_{AB}^{Ad,th}$ stands for the thermal bond opening rate for the adhesin, and where we have used ρ as a short hand notation for the ratio of the lengths of the adhesin and the layer-to-layer bonds, $\Delta x_{AT}^{Ad} / \Delta x_{AT}^{LL}$, respectively.

Since the probability of finding a bond exposed to a constant force in the closed state is given by $\exp(-k_{AB}^{Ad} t)$, the *lifetime* of the adhesin bond in region II, $<\tau>_{II}^{Ad}$, defined as the time after which e^{-1} of all bonds remain in the closed state, can be written as the inverse of the bond opening rate. This implies that it is given by

$$<\tau>_{II}^{Ad} = \frac{1}{k_{AB}^{Ad,th}} e^{-F_{II,UF}^{SS} \Delta x_{AT}^{Ad} / kT} = \frac{1}{k_{AB}^{Ad,th}} e^{-(\Delta x_{AT}^{Ad} / \Delta x_{AB}^{LL}) \Delta V_{AB}^{LL} / kT} \tag{X.13}$$

and

$$<\tau>_{II}^{Ad} = \frac{1}{k_{AB}^{Ad,th}} e^{-F_{II,UF}^{DFS} \Delta x_{AT}^{Ad} / kT} = \frac{1}{k_{AB}^{Ad,th}} \left(\frac{\dot{L}}{\Delta x_{AB}^{LL} k_{AB}^{LL,th}} \right)^{-\rho}, \tag{X.14}$$

for the two cases with $\dot{L} < \dot{L}^*$ and $\dot{L} > \dot{L}^*$, respectively.

For the case when a pilus detaches in region II, it is possible to define an *expected elongation length*, $<L>_{II}^{Ad}$, as the length a pilus can be elongated (in region II) before the adhesin bond opens. Under the condition that the pilus is elongated with a constant elongation speed, this implies that $<L>_{II}^{Ad}$ can be expressed as the product of $<\tau>_{II}^{Ad}$ and the elongation speed, i.e. as

$$\begin{aligned} <L>_{II}^{Ad} = <\tau>_{II}^{Ad} \dot{L} &= \frac{\dot{L}}{k_{AB}^{Ad,th}} e^{-F_{II,UF}^{SS} \Delta x_{AT}^{Ad} / kT} \\ &= \frac{\dot{L}}{k_{AB}^{Ad,th}} e^{-(\Delta x_{AT}^{Ad} / \Delta x_{AB}^{LL}) \Delta V_{AB}^{LL} / kT} \end{aligned} \tag{X.15}$$

and

$$\begin{aligned} <L>_{II}^{Ad} &= \frac{\dot{L}}{k_{AB}^{Ad,th}} e^{-F_{II,UF}^{DFS} \Delta x_{AT}^{Ad} / kT} = \frac{k_{AB}^{LL,th}}{k_{AB}^{Ad,th}} \Delta x_{AB}^{LL} e^{(1-\rho) \frac{F_{II,UF}^{DFS} \Delta x_{AT}^{LL}}{kT}} \\ &= \frac{1}{k_{AB}^{Ad,th}} \frac{\dot{L}^{1-\rho}}{\left(\Delta x_{AB}^{LL} k_{AB}^{LL,th} \right)^{-\rho}}, \end{aligned} \tag{X.16}$$

again for the two cases with $\dot{L} < \dot{L}^*$ and $\dot{L} > \dot{L}^*$, respectively. The expected elongation length under dynamic conditions has in Eq. (X.16) been expressed alterna-

tively in terms of the unfolding force of region II under dynamic conditions, $F_{\mathrm{II,UF}}^{\mathrm{DFS}}$, and the elongation speed, $\dot{L}$. Obviously, these expressions are valid only for the cases when $< L >_{\mathrm{II}}^{\mathrm{Ad}}$ is smaller than the maximal elongated length of the pilus rod, $N_{\mathrm{TOT}}\Delta x_{\mathrm{AB}}^{\mathrm{LL}}$.

If the pilus remains attached into region III, in which the force increases sharply with elongation (and thus time), the probability for detachment will rapidly increase and the pilus will experience a significantly reduced lifetime.

X.4 Results and Discussion

*X.4.1 Typical force-*vs.*-elongation Response of P and Type 1 Pili*

Experiments have been performed on several types of pilus. The biophysical properties of both P and type 1 pili have been assessed in some detail recently by the authors using FMOT [12, 14-24, 36, 37], whereas studies of other types of pilus (e.g. S and F1C) are presently ongoing. Most of the analysis presented here will therefore concern P and type 1 pili. Figure X.6 shows a typical force-*vs.*-elongation response of these two pili for an elongation speed of 0.1 μm/s, with the black and grey curves representing elongation and contraction, respectively.

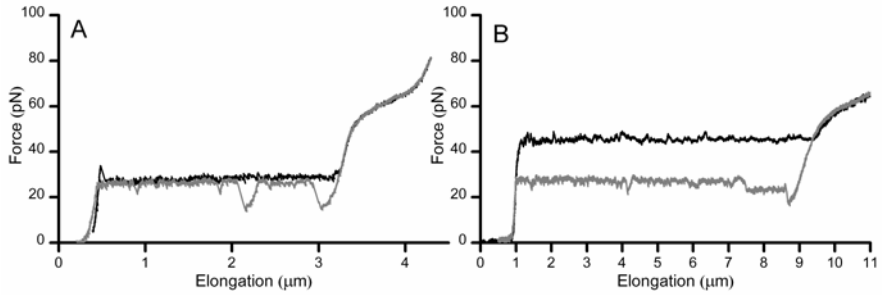

Fig. X.6. Panel A and B show typical single pili responses from a P and a type 1 pili, respectively, for an elongation speed of 0.1 μm/s.

The plateau in region II for P pili, which has almost identical force values for unfolding and refolding (28 ± 2 pN), agrees well with the predicted shape of the force-*vs.*-elongation behavior for unfolding of a helixlike structure under *steady-state* conditions given by Eq. (X.6) and shown in Fig. X.5B. The behavior of type 1 pili, on the other hand, with dissimilar plateau values for unfolding and refolding, shows instead the predicted unfolding response of a helixlike polymer under

dynamic conditions, given by Eq. (X.7). Also the P pili can unfold its quaternary structure under *dynamic* conditions, although this requires higher elongation speeds than 0.1 μm/s [12, 23].

For both types of pilus, region III agrees well with the predicted shape for the elongation of a linear polymer under steady-state conditions, given by Eq. (X.10). By fitting the model equations to curves like those in Fig. X.6, most of model parameters introduced in the models, e.g. ΔV_{AB}^{LL}, ΔV_{BC}^{HT}, Δx_{AB}^{LL}, Δx_{BC}^{HT}, can be assigned values for the two types of pilus.

However, there are two features that cannot be explained by the simple theory given above. The first is the fully reproducible dip in force that appears during contraction following the transition from region III and II. This is considered to be caused by a lack of a nucleation kernel for the formation of a first layer in the quaternary structure during contraction [12, 49]. Occasionally, also other dips in the contraction data can occur, as for example is the case at around 1.5 μm for the P pilus (Fig. X.6A). As is further discussed below, such dips are not reproducible and are considered to originate from sporadic misfoldings not included in the model.

The second feature is the ability of type 1 pili to refold their quaternary structure at two different force levels, ~30 and ~25 pN, respectively, which is illustrated by the gray curve in Fig. X.6B. Although not yet proven, this suggests that type 1 pili can refold into two dissimilar helixlike configurations [21].

Repetitive unfolding and refolding cycles of the PapA rod have furthermore shown that a single P pilus can be elongated and contracted through its entire elongation-and-contraction cycle a large number of times ($> 10^2$) without any alteration of its properties [19]. Such experiments have thus showed that it is possible to elongate a pilus numerous times without any sign of fatigue.

X.4.2 Dynamic Force-vs.-elongation Response

Figure X.7A shows a compilation of some typical force-*vs.*-elongation-speed data for P pili (circles) and type 1 pili (triangles) from measurements such as those shown in Fig. X.6, presented as the unfolding force of region II *vs.* the elongation speed in a lin–log plot. For each type of pili, the data gather in two regions, following two asymptotes; one that is virtually independent of the elongation speed (for low elongation speeds) and one that is linear in a lin–log plot, thus showing an logarithmic behavior (for large elongation speeds). All this is in agreement with the theoretical predictions given in Fig. X.5B above. The two asymptotes meet at the corner velocity. Studies such as these support the model given above and indicate that the corner velocity for the P pili and type 1 pili are significantly different, *viz.* 400 and 6 nm/s, respectively [12].

An example of a study of the dynamic response that follows a sudden halt in elongation is shown in Fig. X.7B together with fits to Eq. (X.8) and it reveals that

the force for P and type 1 pili relaxes to the steady-state force according to Eq. (X.8) for both types of pilus, although with significantly dissimilar speeds for the two types of pilus.

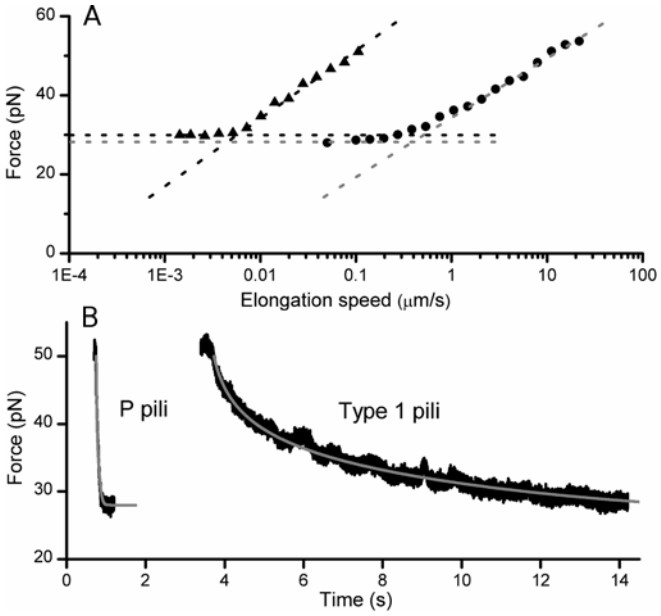

Fig. X.7. Panel A gives the unfolding force in region II of P pili (circles) and type 1 pili (triangles) as a function of (the logarithm of) the elongation speed. The dashed lines represent the low and high elongation speed asymptotes, given by the Eqs (X.6) and (X.7), respectively. The intercept of the two asymptotes represents the corner velocity, $\dot{L}^*$, whereas the intercept of the high elongation speed asymptote with the x-axis gives an entity, $\dot{L}^0$, that provides a value for the thermal bond opening rate, $k_{\mathrm{AB}}^{\mathrm{LL,th}}$. The data for P pili is replotted from Fig. X.5 in Ref. [12]. Panel B shows the response from unfolding of pili under relaxation conditions for P and type 1 pili (with an initial force of 50 pN). The data show that P pili reach their steady-state force after a fraction of a second whereas type 1 pili reach it after ~9 s. Copyright Wiley-VCH Verlag GmbH & Co. KGaA. Reproduced with permission from Ref. [23].

These types of curve can then serve the purpose of assessing values of the bond length and the thermal bond opening rate for the layer-to-layer bond of the two types of pilus, i.e. $\Delta x_{\mathrm{AT}}^{\mathrm{LL}}$ and $k_{\mathrm{AB}}^{\mathrm{LL,th}}$. It was found, for example, that these take the values of 0.76 nm and 0.8 Hz for P pili. The same entities take values of 0.59 nm and 0.016 Hz for type 1 pili.

The examples given in the Figs X.6 and X.7 show that all major properties of the force-*vs.*-elongation behavior of an individual pilus, with the exception of some refolding, have been captured by the simple theory and the expressions given above.

X.4.3 Compilation of Model Parameters and Pili Properties

Table X.1 presents a compilation of some bond parameters that have been assessed for P and type 1 pili. Parameters for other types of pilus, e.g. S and F1C, which are presently under scrutiny, will be presented elsewhere. In addition to measurements on P and type 1 pili performed by the authors [12, 14-18, 21, 36, 37], the table includes some parameters for type 1 pili assessed by Miller *et al.* [50] and Forero *et al.* [51] using force measuring AFM. Note though, to make a comparison possible with the results obtained by the OT-technique, some of their values have been recalculated to agree with the nomenclature used with OT.

Table X.1. Some bond parameters for P and Type 1 pili of *E. coli.*

Parameters	**P pili**	**Type 1**		
Technique	FMOT[a]	FMOT[a]	AFM [50]	AFM [51]
$F_{\mathrm{II,UF}}^{\mathrm{SS}}$ (pN)	28 ± 2	30 ± 2	(60)[b]	22
$k_{\mathrm{AB}}^{\mathrm{LL,th}}$ (Hz)	0.8 ± 0.5	0.016 ± 0.009	0.05	0.5
$k_{\mathrm{AB}}^{\mathrm{LL,bal}}$ (Hz)	120 ± 75	1.2 ± 0.9	0.8	2.2
$\dot{L}^{*}$ (nm/s)	400	6		
$\Delta V_{\mathrm{AT}}^{\mathrm{LL}}$ (kT)	23 ± 1	27 ± 2	26[c]	29
$\Delta V_{\mathrm{AB}}^{\mathrm{LL}}$ (kT)	24 ± 1	37 ± 2	16[c]	25
$\Delta x_{\mathrm{AT}}^{\mathrm{LL}}$ (nm)	0.76 ± 0.11	0.59 ± 0.06	0.2	0.26 ± 0.01
$\Delta x_{\mathrm{AB}}^{\mathrm{LL}}$ (nm)	3.5 ± 0.1			5 ± 0.3

[a] Refs [12, 14-18, 21, 36, 37]. [b] Measured at 1-3 μm/s, which, according to FMOT measurements, is not at steady-state. [c] Recalculated using at an attempt rate of 10^{10} Hz.

It is known from scanning transmission electron microscopy that many types of pilus have structural similarities [9]. Although measurements of their physical properties to a certain extent have shown similar behaviors, they have also revealed striking differences. It has, for example, been found that the steady-state unfolding forces of the quaternary structure of P and type 1 pili, $F_{\mathrm{II,UF}}^{\mathrm{SS}}$, are comparable, 28 ± 2 pN and 30 ± 2 pN, respectively.[1] On the other hand, presently ongoing work (unpublished results) has shown that other types of pilus, e.g. F1C, have significantly lower steady-state unfolding forces, < 10 pN.

[1] The reported unfolding force of type 1 pilus by Miller *et al.* [50] of 60 pN was performed for an elongation speed of 1-3 μm/s. Since this is significantly higher than the corner frequency, $\dot{L}^{*}$, their value is assumed to be an assessment of the unfolding force under dynamic conditions.

Moreover, the thermal bond opening rate, $k_{AB}^{LL,th}$, for P pili has been assessed to 0.8 ± 0.5 Hz [12] which is significantly larger (~ 50 times) than that for type 1 pili, which has been assessed to 0.016 ± 0.009 Hz. This implies that the layer-to-layer bonds for P pili open, and thereby close, thermally much more often than those for type 1 pili. This is also in agreement with the fact that the balance rate and the corner velocity are significantly larger for P pili than for type 1 pili ($k_{AB}^{LL,bal}$ is 120 *vs.* 1.2 Hz, whereas $\dot{L}^*$ is 400 *vs.* 6 nm/s for the two types of pili, respectively). This indicates that that P pili reach their stationary force balance (i.e. $F_{II,UF}(\dot{L}=0)$) much faster than type 1 pili. Moreover, since the thermal bond opening rate, $k_{AB}^{LL,th}$, can be written as $\nu \exp(-\Delta V_{AT}^{LL}/kT)$, the two-orders-of-magnitude difference in $k_{AB}^{LL,th}$ indicates (under the condition that the attempt rates are the same) that the layer-to-layer bonds in type 1 pili have an activation energy that is 4 *kT* larger than that of P pili (27 *kT* and 23 *kT,* respectively).

How a pilus reacts to stress is not only given by the height of the transition state, also the bond length, Δx_{AT}^{LL}, affects the functioning of a bond. It has been found that the layer-to-layer bond length is longer for P pili than for type 1 pili (0.76 ± 0.11 *vs.* 0.59 ± 0.06 nm). [2] This implies that the transition barrier for type 1 pili is both higher and steeper than for P pili. This is in line with the fact that type 1 pili have a slower thermal unfolding rate than P pili and suggests that they are less sensitive to external forces.

It is interesting to note that the bond opening energy of the layer-to-layer bonds of both P and type 1 pili, ΔV_{AB}^{LL}, which were assessed to 24 *kT* and 37 *kT* respectively, are *larger* than those of the transition barriers, ΔV_{AT}^{LL}, 23 *kT* and 27 *kT,* respectively.[3] This implies that neither type 1 pili, nor P pili, possesses a bound unfolded state in the absence of force, as was schematically indicated in Fig. X.4. There is therefore no activation energy for bond closure in the absence of force. This implies that whenever a bond has opened spontaneously, it will close directly (with the attempt rate). None of the structures will therefore be found in an unfolded state unless an external force is applied. Hence, static images of unfolded pili are most likely a result of the treatment during preparation.

X.4.5 Bacterial Detachment under Stress

As was mentioned above, experiments performed on multi-pili bacterial adhesion under stress will not give an unambiguous picture of the fundamental interactions

---

[2] The value of the bond length of type 1 pili assessed by FMOT (0.59 ± 0.06 nm), was found to be significantly larger than that estimated from AFM studies (0.26 ± 0.01 nm) [51]. We have presently no explanation to this discrepancy.

[3] The bond opening energy of the layer-to-layer bonds for type 1 pili is in reasonable, although not perfect, agreement with those assessed for type 1 pili by AFM, 26 *kT* (recalculated from 17 *kT* with an attempt rate of 10^6 to an attempt rate of 10^{10} Hz which has been used throughout this work) by Miller *et al.* [50] and 29 *kT* reported by Forero *et al.* [51].

in the system, primarily due to a partly unknown interplay between various pili. It is therefore necessary to first acquire a full understanding of the combined elongation and adhesion properties of a single pilus. Whence this has been done, it is possible to model how individual pili act cooperatively in order to sustain a shear force and thereby contribute to the ability for a multi-pili-binding bacterium to sustain the rinsing action of shear flow. Such models can then be compared to findings from multi-pili experiments for verification. However, although the characterization of the elongation properties of various pili has been done during the last years, and is still under way, investigations of the properties of the adhesin have only recently been done. There is so far only a limited amount of data about this phenomenon available. No full description of the combined action of rod and adhesin for the total adhesive properties of a single pilus has therefore yet been developed. On the other hand, based upon the models of elongation-and-contraction of pili under stress that recently have been derived, e.g. those given in the Sects X.3.1 – X.3.3 above, it is still possible to hypothesize how the rod and the adhesin of a single pilus jointly act in response to an external force as well as the expected response from a multi-pili attachment. Such hypotheses can then be verified by experiments.

X. 4.5.1 Single Pilus Detachment

Section X. 3.5 above provided expressions for the expected adhesion lifetime and elongation length of a pilus elongated in region II. For the case with low elongation speed, i.e. when $\dot{L} < \dot{L}^*$, the expected adhesion lifetime is given by Eq. (X.13), whereas the expected elongation length is given by Eq. (X.15). These expressions indicate that for low speeds, i.e. for $\dot{L} < \dot{L}^*$, the adhesion lifetime is independent of the elongation speed and the expected elongation length is directly proportional to the elongation speed. This implies that the faster a pilus is elongated in region II (although still for $\dot{L} < \dot{L}^*$), the longer it can be elongated before being detached.

In the high speed elongation case, $\dot{L} > \dot{L}^*$, on the other hand, the Eq. (X.14) indicates that the expected lifetime of a single pilus decreases with increasing elongation speed, which is the normal behaviour of a single bond. However, Eq. (X.16) shows that the expected elongation length is independent of the force for the case when the lengths of the layer-to-layer and the adhesin bonds are equal. Interestingly, it also shows that if the bond length for the adhesin is shorter than that for the layer-to-layer bond (i.e. $\rho < 1$), the expected elongation length *increases* with force. For other cases the expected elongation length will scale exponentially with the applied force.

It has recently been found in an ongoing work (unpublished results), performed at three different speeds, and thereby for three different unfolding forces, that the expected elongation length for the PapG-galabiose binding of P pili indeed increases with the applied force, as suggested by this hypothesis. This implies, according to Eq. (X.16), that the length of the adhesin bond is shorter than that of the

layer-to-layer bond for P pili, i.e. $\rho < 1$. It also implies that the higher the loading rate, the longer the pilus will be elongated before it detaches. This increases, in turn, the possibility for the bacterial system to adopt a multi-pili binding (since other pili might become elongated into their region II before the adhesin of the first pilus rupture).

It has been shown recently that the typical lifetime of a PapG-galabiose bond, when exposed to the steady-state unfolding force (28 pN), is in the order of 10 s [48]. Since the corner velocity for a P pilus is 0.4 μm/s, and the length of region II is typically a few μm, it can be estimated that a single P pilus exposed to the steady-state unfolding force and elongated at an elongation speed close to the corner velocity will have a reasonable chance of detaching in region II. If the elongation is performed at a slower pace, the probability for detachment during the elongation in region II will increase. On the other hand, if the pilus does not detach in region II, it will enter region III where the force increases rapidly. This implies that the adhesin bond will open reasonably fast (within a time $\ll$ 10 s).

X.4.5.2 Multi-pili Detachment

Multi-pili attachment is presumably of more importance than single-pilus attachment since this allows for an external force, F_{ext}, to be distributed among a multitude of pili. The exact distribution of forces will depend on a number of factors, e.g. the number of pili as well as their lengths and surface distribution, wherefore only some general conclusion will be drawn here.

As long as the number of pili is sufficiently large, primarily above $F_{\text{ext}} / F_{\text{II,UF}}$, no pili will be elongated into region III. If the force is above $F_{\text{II,UF}}$, it will redistribute among several pili elongated either into region I or II. All pili in region II (N_{II}) will then experience the same expected lifetime, namely $< \tau >_{\text{AB}}^{\text{Ad}}$, given by either Eq. (X.13) or (X.14). The expected lifetime before the first pilus detaches is then given roughly by $< \tau >_{\text{AB}}^{\text{Ad}} / N_{\text{II}}$. When one pilus has detached, the force will be rapidly redistributed among the remaining pili. As long as there are a sufficient number of pili remaining, this procedure will be repeated.

However, when the remaining pili are few, approximately below $F_{\text{ext}} / F_{\text{II,UF}}$, at least one pilus will be elongated into region III, whereby it will experience a significantly shorter lifetime. When this takes place, there will be a rapid sequence of pili detachments, until the entire bacterium is detached.

Moreover, multi-pili attachment is far from intuitive. For example, if the first pilus to support the force is being elongated rapidly (i.e. into its dynamic regime), it is possible that a second pilus can become elongated and take up some of the force before the first pilus detaches. The force will then be distributed among the two pili, which, in turn, leads to detachment rates for the two pili that are lower than that of the first pilus elongated slowly. A fast elongation can therefore give rise to a longer lifetime time for bacterial adhesion than a slow elongation.

The details of multi-pili attachment have just recently been understood, and work is therefore presently in progress to characterize these important phenomena.

It is clear though that multi-pili mechanism can induce a strong binding to the host cells and may be an important key for the rinsing-resistance of a bacterium.

X.5 Summary and Conclusions

Two types of uropathogenic *E. coli* bacterial pili, P and type 1, which are predominantly expressed by *E. coli* in the upper and lower urinary tracts, have been scrutinized in some detail using force measuring optical tweezers (FMOT). A model for the bond opening of the layer-to-layer bond in the helixlike structure as well as the opening of the head-to-tail bond between consecutive subunits in the rod, based upon an energy landscape model and a kinetic model (of sticky-chain type) for the bond opening, has been developed. It has been possible to characterize virtually all parameters in this model by the use of single pilus force-*vs*.-elongation measurements on individual pili. This has given rise to a model for the elongation properties of a single pilus under strain/stress. Lately, also information about the adhesin at the tip of the attachment organelle has been assessed. The first steps towards a combined description of the elongation and adhesion properties of pili-expressed bacterial adhesion have thereby been taken. This analysis indicates that the unique properties of the pili provide the bacteria with an extraordinary ability to sustain significant shear forces, forces that can widely supersede the binding force of a single (non-piliated) adhesin. Moreover, the results for the different pili provide information that presumably can be correlated to the particular environment in which they are found. For example, the steeper potential of type 1 pili may be considered a consequence of the fact that the structure has evolved to support higher forces during shorter time events, which would correlate with the irregular urine flow in the bladder and the urethra as compared to the more constant urine flow in the upper urinary tracts. It is therefore possible that the much stiffer bond potential for type 1 pili is optimized for a fast shock damping effect. All this indicates that different types of pilus can have significantly dissimilar biophysical properties and that they therefore presumably are optimized for dissimilar environments.

Further work with other pili as well as analysis of multi-pili responses of the studied systems is on its way. With this information at hand, a significantly improved understanding of adhesion by piliated bacteria can be gained. Based upon this knowledge the search for new targets for anti-adhesion drugs in bacteria which possibly could lead to new means to combat bacterial infections, including those from antibiotic resistant bacterial strains [20, 52, 53], can be initiated.

Acknowledgements

This work was supported by the Swedish Research Council under the project 621-2005-4662 and performed within the Umeå Centre for Microbial Research (UCMR). The authors acknowledge economical support for the construction of a force-measuring optical tweezers system from the Kempe foundation and from Magnus Bergvall's foundation. The "Fondation Pour La Recherche Médicale" is also acknowledged for the French post-doctoral fellowship awarded to Mickaël Castelain (grant no. SPE20071211235).

References

[1] Thomas W.E., Trintchina E., Forero M., Vogel V. and Sokurenko E.V.: Bacterial adhesion to target cells enhanced by shear force, Cell. **109**, 913-923 (2002)

[2] Anderson B.N., Ding A.M., Nilsson L.M., Kusuma K., Tchesnokova V., Vogel V., Sokurenko E.V. and Thomas W.E.: Weak Rolling Adhesion Enhances Bacterial Surface Colonization, 10.1128/JB.00899-06, J. Bacteriol. **189**, 1794-1802 (2007)

[3] Jacobdubuisson F., Heuser J., Dodson K., Normark S. and Hultgren S.: Initiation of Assembly and Association of the Structural Elements of a Bacterial Pilus Depend on 2 Specialized Tip Proteins, EMBO J. **12**, 837-847 (1993)

[4] Johnson J.R. and Russo T.A.: Uropathogenic Escherichia coli as agents of diverse non-urinary tract extraintestinal infections, J. Infect. Dis. **186**, 859-864 (2002)

[5] Russo T.A. and Johnson J.R.: Medical and economic impact of extraintestinal infections due to Escherichia coli: focus on an increasingly important endemic problem, Microbes Infect. **5**, 449-456 (2003)

[6] Källenius G., Svenson S.B., Hultberg H., Möllby R., Helin I., Cedergren B. and Winberg J.: Occurrence of P-fimbriated Escherichia coli in urinary tract infections, Lancet. **2**, 1369-1372 (1981)

[7] Ruiz J., Simon K., Horcajada J.P., Velasco M., Barranco M., Roig G., Moreno-Martinez A., Martinez J.A., de Anta T.J., Mensa J. and Vila J.: Differences in virulence factors among clinical isolates of Escherichia coli causing cystitis and pyelonephritis in women and prostatitis in men, J. Clin. Microbiol. **40**, 4445-4449 (2002)

[8] Bullitt E. and Makowski L.: Structural polymorphism of bacterial adhesion pili, Nature. **373**, 164 -167 (1995)

[9] Hahn E., Wild P., Hermanns U., Sebbel P., Glockshuber R., Haner M., Taschner N., Burkhard P., Aebi U. and Muller S.A.: Exploring the 3D molecular architecture of Escherichia coli type 1 pili, J. Mol. Biol. **323**, 845-857 (2002)

[10] Forero M., Thomas W.E., Bland C., Nilsson L.M., Sokurenko E.V. and Vogel V.: A catch-bond based nanoadhesive sensitive to shear stress, Nano Letters. **4**, 1593-1597 (2004)

[11] Lund B., Lindberg F., Marklund B.I. and Normark S.: The Papg Protein Is the Alpha-D-Galactopyranosyl-(1- 4)-Beta-D-Galactopyranose-Binding Adhesin of Uropathogenic Escherichia-Coli, Proceedings of the National Academy of Sciences of the United States of America. **84**, 5898-5902 (1987)

[12] Andersson M., Fällman E., Uhlin B.E. and Axner O.: Dynamic force spectroscopy of the unfolding of P pili, Biophys. J. **91**, 2717-2725 (2006)

[13] Thomas W.E., Nilsson L.M., Forero M., Sokurenko E.V. and Vogel V.: Shear-dependent 'stick-and-roll' adhesion of type 1 fimbriated Escherichia coli, Mol. Microbiol. **53**, 1545-1557 (2004)

[14] Jass J., Schedin S., Fällman E., Ohlsson J., Nilsson U., Uhlin B.E. and Axner O.: Physical properties of Escherichia coli P pili measured by optical tweezers, Biophys. J. **87**, 4271-4283 (2004)

[15] Fällman E., Andersson M., Schedin S., Jass J., Uhlin B.E. and Axner O.: Dynamic properties of bacterial pili measured by optical tweezers, SPIE. **5514**, 763-733 (2004)

[16] Fällman E., Schedin S., Jass J., Uhlin B.E. and Axner O.: The unfolding of the P pili quaternary structure by stretching is reversible, not plastic, EMBO Rep. **6**, 52–56 (2005)

[17] Andersson M., Fällman E., Uhlin B.E. and Axner O.: A sticky chain model of the elongation of Escherichia coli P pili under strain, Biophys. J. **90**, 1521-1534 (2006)

[18] Andersson M., Fällman E., Uhlin B.E. and Axner O.: Technique for determination of the number of PapA units in an E coli P pilus, SPIE. **6088**, 326-337 (2006)

[19] Andersson M., Axner O., Uhlin B.E. and Fällman E.: Optical tweezers for single molecule force spectroscopy on bacterial adhesion organelles, SPIE. **6326**, 1-12 (2006)

[20] Aberg V., Fallman E., Axner O., Uhlin B.E., Hultgren S.J. and Almqvist F.: Pilicides regulate pili expression in E-coli without affecting the functional properties of the pilus rod, Mol. Biosyst. **3**, 214-218 (2007)

[21] Andersson M., Uhlin B.E. and Fällman E.: The biomechanical properties of E. coli pili for urinary tract attachment reflect the host environment, Biophys. J. **93**, 3008-3014 (2007)

[22] Bjornham O., Axner O. and Andersson M.: Modeling of the elongation and retraction of Escherichia coli P pili under strain by Monte Carlo simulations, European Biophysics Journal with Biophysics Letters. **37**, 381-391 (2008)

[23] Andersson M., Axner O., Almqvist F., Uhlin B.E. and Fallman E.: Physical properties of biopolyrners assessed by optical tweezers: Analysis of folding and refolding of bacterial pili, Chemphyschem. **9**, 221-235 (2008)

[24] Andersson M. and Fällman E.: Characterization of S pili - investigation of their biomechanical properties, Biophys. J. Submitted for publication (2007)

[25] Neuman K.C. and Block S.M.: Optical trapping, Rev. Sci. Instr. **75**, 2787-2809 (2004)

[26] Ashkin A.: Acceleration and trapping of particles by radiation pressure, Phys. Rev. Lett. **24**, 156-159 (1970)

[27] Ashkin A.: Optical levitation by radiation pressure, Appl. Phys. Lett. **19**, 283-285 (1971)

[28] Ashkin A., Dziedzic J.M., Bjorkholm J.E. and Chu S.: Observation of a single beam gradient force optical trap for dielectric particles, Opt. Lett. **11**, 288-290 (1986)

[29] Lang M.J. and Block S.M.: Resource letter: LBOT-1: Laser-based optical tweezers, American Journal of Physics. **71**, 201-215 (2003)

[30] Block S.M.: Making light work with optical tweezers, Nature. **360**, 493-495 (1992)

[31] Svoboda K. and Block S.M.: Biological applications of optical forces, Annu. Rev. Biophys. Biomem. **23**, 247-285 (1994)

[32] Greenleaf W.J., Woodside M.T., Abbondanzieri E.A. and Block S.M.: Passive all-optical force clamp for high-resolution laser trapping, Phys. Rev. Lett. **95**, (2005)

[33] Bustamante C., Macosko J.C. and Wuite G.J.L.: Grabbing the cat by the tail: Manipulating molecules one by one, Nature Reviews Molecular Cell Biology. **1**, 130-136 (2000)

[34] Bustamante C., Bryant Z. and Smith S.B.: Ten years of tension: single-molecule DNA mechanics, Nature. **421**, 423-427 (2003)

[35] Fällman E. and Axner O.: Design for fully steerable dual-trap optical tweezers, Appl. Opt. **36**, 2107-2113 (1997)

[36] Fällman E., Schedin S., Jass J., Andersson M., Uhlin B.E. and Axner O.: Optical tweezers based force measurement system for quantitating binding interactions: system design and application for the study of bacterial adhesion, Biosens. Bioelectron. **19**, 1429-1437 (2004)

[37] Andersson M., Fällman E., Uhlin B.E. and Axner O.: Force measuring optical tweezers system for long time measurements of Pili stability, SPIE. **6088**, 286-295 (2006)

[38] Gittes F. and Schmidt G.F.: Signals and noise in micromechanical measurements, Methods in Cell Biology. **55**, 129-156 (1998)

[39] Bell M.G.: Models for the specific adhesion of cells to cells, Science. **200**, 618-627 (1978)

[40] Evans E.: Probing the relation between force - lifetime - and chemistry in single molecular bonds, Annu. Rev. Biophys. Biomem. **30**, 105-128 (2001)

[41] Evans E. and Ritchie K.: Dynamic strength of molecular adhesion bonds, Biophys. J. **72**, 1541-1555 (1997)

[42] Evans E.: Energy landscapes of biomolecular adhesion and receptor anchoring at interfaces explored with dynamic force spectroscopy, Faraday Discussions. 1-16 (1998)

[43] Evans E.: Looking inside molecular bonds at biological interfaces with dynamic force spectroscopy, Biophys. Chem. **82**, 83-97 (1999)

[44] Evans E. and Ritchie K.: Strength of a weak bond connecting flexible polymer chains, Biophys. J. **76**, 2439-2447 (1999)

[45] Jäger I.: The "sticky chain": A kinetic model for the deformation of biological macromolecules, Biophys. J. **81**, 1897-1906 (2001)

[46] Merkel R., Nassoy P., Leung A., Ritchie K. and Evans E.: Energy landscapes of receptor-ligand bonds explored with dynamic force spectroscopy, Nature. **397**, 50-53 (1999)

[47] Strunz T., Oroszlan K., Schumakovitch I., Guntherodt H.J. and Hegner M.: Model energy landscapes and the force-induced dissociation of ligand-receptor bonds, Biophys. J. **79**, 1206-1212 (2000)

[48] Nilsson H., *"P pili elongation generates a dynamic force response suggesting a slip-bond mechanism for the PapG-Galabiose adhesin-receptor pair,"* Master thesis, Umeå University, 2008.

[49] Lugmaier R.A., Schedin S., Kuhner F. and Benoit M.: Dynamic restacking of Escherichia coli P-pili, European Biophysics Journal with Biophysics Letters. **37**, 111-120 (2008)

[50] Miller E., Garcia T.I., Hultgren S. and Oberhauser A.: The Mechanical Properties of E. coli Type 1 Pili Measured by Atomic Force Microscopy Techniques, Biophys. J. **91**, 3848-3856 (2006)

[51] Forero M., Yakovenko O., Sokurenko E.V., Thomas W.E. and Vogel V.: Uncoiling Mechanics of Escherichia coli Type I Fimbriae Are Optimized for Catch Bonds, PLoS Biology. **4**, 1509-1516 (2006)

[52] Svensson A., Larsson A., Emtenas H., Hedenstrom M., Fex T., Hultgren S.J., Pinkner J.S., Almqvist F. and Kihlberg J.: Design and evaluation of pilicides: Potential novel antibacterial agents directed against uropathogenic Escherichia coli, Chembiochem. **2**, 915-918 (2001)

[53] Åberg V. and Almqvist F.: Pilicides—small molecules targeting bacterial virulence, Organic and Biomolecular Chemistry. **5**, 1827-1834 (2007)

Index